Electronic structure and optical properties of metallic calcium*

Daniel J. Mickish,† A. Barry Kunz, and Sokrates T. Pantelides‡
Department of Physics and Materials Research Laboratory, University of Illinois at Urbana-Champaign, Urbana, Illinois 61801
(Received 15 October 1973)

Self-consistent Hartree-Fock orbitals of calcium atoms in a crystalline environment were used in conjunction with the localized linear-combination-of-atomic-orbital method to obtain one-electron bands for metallic calcium. Correlation corrections are made by means of Overhauser's simplified method. The metal-to-semimetal-to-metal electronic transitions with increasing pressure are predicted to occur at smaller lattice spacings than predicted by calculations employing local exchange. A rigorous calculation of ϵ_2, the imaginary part of complex dielectric function, made within the dipole and one-electron approximation predicts correctly the general shape and width of the $1s$-valence emission spectra and the important structures superimposed on the broad $1s$-conduction absorption spectra. There is good agreement with the specific-heat data, but the details of the Fermi surface as described by de Haas–van Alphen data have remained elusive—large percentage errors occur when the predicted areas are compared with the experimental results. The de Haas–van Alphen orbit areas are extremely sensitive to the accuracy of the calculations due to the flatness of the bands near the Fermi level.

I. INTRODUCTION

The purpose of this paper is to present rigorous Hartree-Fock energy bands for a real metal. The metal calcium has been chosen in order to exploit its atomic closed-shell properties and to use its metal to semimetal electronic transition properties observed under increasing pressure as a test of the accuracy of Hartree-Fock bands. Additional tests are made using available optical and de Haas–van Alphen data.

Nearly all calculations to date made on metals have approximated the true Hartree-Fock nonlocal exchange through the use of the formalism of Hohenberg, Kohn, and Sham.[1,2] Their work establishes the existence of a universal functional of the local density of an interacting electron gas which is capable of providing the correlated ground-state energy of the system, provided that the ground state is nondegenerate. Gilbert[3] has recently shown that if the external potential is nonlocal then the energy is a unique functional of the density operator, not the local density. This is a severe restriction since it complicates the use of local exchange potentials in real crystals as a means of obtaining arbitrarily accurate solutions. If (nonlocal) ion-core external potentials are used, then local exchange potentials are incapable of describing the true exchange. If, however, (local) nuclear external potentials are used, then the exchange potentials proportional to the local density to the one-third power[2,4–6] are not accurate since they require that the external potential be slowly varying.

In order to achieve a higher degree of accuracy in calculations of the electronic structure of solids one is faced with two known choices. The first choice involves the retaining of the Hohenberg-Kohn[1] theorem and the search for a universal functional of the electron density which is far from slowly varying. There is no way of determining this functional, *a priori*, other than by using a functional expansion starting from the approximate expression valid for a homogeneous electron gas at high densities. The expansion must be capable of describing the effects of the singular Coulomb potentials which occur in real materials. The second choice involves the use of the well-known functional

$$E[\psi] = \langle\psi|H|\psi\rangle / \langle\psi|\psi\rangle$$

and systematic approximations in the application of this functional. Although at first thought this approach may lead to elaborate and tedious calculations, we have found that through the use of powerful mathematical transformations such as those that exist in local orbitals theory[7–14] and the efficient use of the random-access capabilities of modern computers, the second choice of attack is fully competitive with the first in terms of computation time.

The results presented in this paper were obtained by first making a one-electron approximation to $E[\psi]$ and minimizing the energy leading to self-consistent Hartree-Fock Bloch eigenfunctions and energies. Several groups[7–22] have developed mathematical and computational techniques which allow rather accurate determination of the Hartree-Fock bands for a variety of crystals. The agreement among the various Hartree-Fock bands obtained by the different techniques is very good in spite of the use of approximations such as muffin-tin potentials in some cases and the wide diversity of basis functions employed.[15] Crystalline Hartree-Fock Bloch functions may be used as zero-order wave functions to accurately calculate the correlation energy as in Kunz's[23] method based on Toyo-

TABLE I. Exponents and coefficients of Slater-type basis functions (STO's) used to construct self-consistent Hartree-Fock local orbitals for the equilibrium lattice: $\phi_{ai}=\sum_\lambda C_{ai,\lambda}\chi_\lambda$. Coefficients to be used for "virtual" orbitals are indicated by an asterisk.

λ	STO χ_λ	Exponent	$C_{1s,\lambda}$	$C_{2s,\lambda}$	$C_{3s,\lambda}$	$C_{4s,\lambda}$	$C^*_{5s,\lambda}$	$C^*_{6s,\lambda}$	$C^*_{7s,\lambda}$
1	1s	20.0000	0.97737	0.28339	0.09749	0.00450	0.0	0.0	0.0
2	3s	22.0757	0.02629	0.00390	0.00016	0.01387	0.0	0.0	0.0
3	3s	15.1048	0.01113	−0.19536	−0.06793	−0.06203	0.0	0.0	0.0
4	3s	9.9852	−0.00192	0.61682	−0.24971	0.15126	0.0	0.0	0.0
5	3s	7.2167	0.00102	−0.27025	−0.19569	−0.22970	0.0	0.0	0.0
6	3s	3.7902	0.00036	−0.00467	−0.68237	0.41196	0.0	0.0	0.0
7	3s	2.5921	0.00014	0.00001	0.47653	−0.40514	0.0	0.0	0.0
8	4s	1.4168	−0.00003	−0.00012	−0.00077	0.66866	0.0	0.0	0.0
9	4s	0.8587	0.00001	0.00005	0.00257	−1.40270	0.0	0.0	0.0
10	4s	1.3500	0.0	0.0	0.0	0.0	1.0	0.0	0.0
11	5s	1.5200	0.0	0.0	0.0	0.0	0.0	1.0	0.0
12	6s	1.6800	0.0	0.0	0.0	0.0	0.0	0.0	1.0

			$C_{2p,\lambda}$	$C_{3p,\lambda}$	$C^*_{4p,\lambda}$	$C^*_{5p,\lambda}$
1	2p	10.0000	0.67883	0.22133	0.0	0.0
2	4p	17.3718	0.01298	0.00284	0.0	0.0
3	4p	10.4808	0.24110	0.07190	0.0	0.0
4	4p	7.5803	0.15816	−0.00661	0.0	0.0
5	4p	4.7717	0.00239	−0.46585	0.0	0.0
6	4p	2.9791	0.00100	−0.55991	0.0	0.0
7	4p	1.8414	−0.00024	−0.06887	0.0	0.0
8	3p	1.2200	0.0	0.0	1.0	0.0
9	4p	1.4000	0.0	0.0	0.0	1.0

			$C^*_{3d,\lambda}$	$C^*_{4d,\lambda}$
1	3d	1.2200	1.0	0.0
2	4d	1.4000	0.0	1.0

zawa's[24] electronic polaron. Semiclassical methods for determining the correlation corrections can also be implemented in the case of insulators. These include the Mott-Littleton[25] method and the screened-exchange-plus-Coulomb-hole method.[26] The resulting correlated bands closely match experiment for the cases which they have been calculated.[16,26] In the case of metals, a simplified theory of electron correlation by Lundquist and Overhauser[27,28] may be used to correct the Hartree-Fock bands. Of course, the inclusion of correlation corrections via the well-known techniques of multiconfiguration self-consistent-field[29] or configuration interaction[30] is a definite possibility, although no such calculation has been performed on a crystalline material. It is interesting to note that the only approximation to the exchange operator that does give eigenvalues close to the Hartree-Fock values is Liberman's[31,32] energy-dependent excitation Hamiltonian.

II. CALCULATION

A. Local orbitals, Bloch eigenfunctions, and bands

The local orbitals equation[7-9,11] used in this paper

$$(F_a + U_a - \rho U_a \rho)\,|\phi_{ai}\rangle = \epsilon_{ai}\,|\phi_{ai}\rangle \qquad (1)$$

has been evaluated self-consistently to first order in overlap as indicated by Kunz.[13] The operator F_a is that part of the Hartree-Fock operator which involves only center a and U_a is simply the remainder, which can be considered as the potential field produced by the environment.

The appropriateness of retaining terms to only first order in overlap has been rigorously studied in a recent work by Kunz.[33] It was found that the approximation was justified even in some covalently bonded systems and, therefore, we believe that it is certainly justified in the present case of the calcium system.

Basis functions used for the determination of local orbitals for calcium were obtained from an earlier very accurate calculation of the atom.[34] The atomic eigenfunctions were used to begin the iteration process. The local orbitals are given in Table I. Also appearing in the table are the additional orbitals which were included to allow description of the unoccupied conduction band levels. The equilibrium lattice constant a_0 was taken as 10.54 bohr (5.58 Å).

The last iteration in the search for self-consistency involved the determination of Bloch eigenfunctions rather than a new set of local orbitals. The Bloch basis consisted of linear combinations

of self-consistent local orbitals and compact Slater-type orbitals (STO's). This method can be considered a complete generalization of the linear-combination-of-atomic-orbitals (LCAO) method.[15,22,35-37] There are two significant advantages to using the LCAO method. First, the local orbitals completely span the occupied Hartree-Fock space (assuming no approximations were invoked) and so basis functions built as Bloch sums of the local orbitals will also span that space. Second, the resulting integrals over local orbitals are independent of the crystal momentum $\vec{k}$. Once the integrals are determined for diagonalizing $F = F_a + U_a$ at any one point in the Brillouin zone, the same integrals can be used with only a change in multiplying phase factors to diagonalize F at any other point. This method has proved to be the most economical, since evaluation of the bands is required at a large number of points in the Brillouin zone in order to make adequate comparisons with experimental optical and de Haas–van Alphen data.

There are some interesting concepts involved in going from the closed-shell calcium atom to the "open-shell" calcium metal when using the local orbitals and LCAO techniques. We wish to first point out that the local orbitals equation [Eq. (1)] possesses the point group symmetry of the crystal (O_h in the present case) and therefore the eigenfunctions $|\phi_{ai}\rangle$ will transform according to the irreducible representation of that point group. The self-consistent density matrix is determined by an expression constructed of local orbitals (LO):

$$\rho_{\mathrm{LO}}(\vec{r},\vec{r}') = \sum_{ai,bj} |\phi_{ai}(\vec{r})\rangle S^{-1}_{ai,bj} \langle\phi_{bj}(\vec{r}')| \ . \qquad (2)$$

This form of the density matrix is completely equivalent[7,8] to the canonical Hartree-Fock matrix

$$\rho(\vec{r},\vec{r}') = \sum_{n,\vec{k}} |\psi_{n,\vec{k}}(\vec{r})\rangle\langle\psi_{n,\vec{k}}(\vec{r}')| \ , \qquad (3)$$

where the ψ's are eigenfunctions of the Hartree-Fock operator. There does exist a somewhat pathological case where the restricted Hartree-Fock approximation fails to be adequate, causing the breakdown of the equivalence of Eqs. (2) and (3). This occurs when the free atomic system can be described as closed shell but the fragment (here the atom in a crystal field) cannot be described as a set of closed-shell local orbitals. In the case of calcium this situation would manifest itself by an apparent crossing of the free atomic–local orbital energy levels. The atomic $3d$ level, for example, could split into $\Gamma_{25'}$ and Γ_{12} levels with the $\Gamma_{25'}$ crossing the $4s$-Γ_1 level such that it would lie below the Γ_1 level. When the local orbitals are filled according to the energy criteria, the last two $4s$ electrons would be assigned to the lower $\Gamma_{25'}$ degenerate level instead of the usual Γ_1 level giving rise to an open shell and not treatable by means of restricted Hartree-Fock. Although we have not explicitly carried out an open-shell local-orbitals calculation on calcium, we believe that the very large (1.25 Ry) energy difference between Γ_1 and $\Gamma_{25'}$ obtained from the equilibrium bands (Fig. 1) supports the assumption that the local orbitals level $\Gamma_{25'}$ does not lie below Γ_1 and that the local-orbital system is therefore closed.

Second, we wish to point out that in the present case the environment U_a used in the local orbitals Eq. (1) is approximated by the first term of its expansion in cubic harmonics. The first term possesses spherical symmetry (the second Y_4^m symmetry) and so the solutions to the local-orbitals equation transform according to the irreducible representations of the three dimensional rotation group. The density matrix is now constructed of local orbitals $|\phi_{ai}\rangle$ which have only pure s and pure p symmetry. We now indicate to what degree this "spherical approximation" to U_a causes Eq. (2) to differ from Eq. (3). Of special concern is the realization that some states having d-like or higher symmetry must be occupied since the $4s$ and $3d$ or higher atomic levels must merge to obtain metallic behavior in the crystal. The states near the Fermi level (e.g., X_1, L_1, U_1, W_2', K_1), however, possess very little d like or higher symmetries being composed of mostly s- and p-like symmetry. A qualitative measure of the number of d-like or higher states making up the occupied orbitals can be determined by the degree to which bands from the second Brillouin zone lie below the Fermi level. As seen in Fig. 1, there are few states from the second zone lying below the Fermi level.

We therefore maintain that although $\rho_{\mathrm{LO}}(\vec{r},\vec{r}')$ only approximates $\rho(\vec{r},\vec{r}')$ due to the spherical approximation to U_a, the approximation is extremely good. In addition, the last operation of determining the Bloch eigenfunctions from $\rho_{\mathrm{LO}}(\vec{r},\vec{r}')$ is effectively a final iteration toward self-consistency without spherical symmetrization of U_a. Any resulting ψ's partially containing Bloch sums of d-like STO's are permitted to be occupied if energetically favorable. As a consequence bands describing metallic behavior are found (see Fig. 1, $a/a_0 = 1.0$).

Two technical points are in order. Exponents of the STO's used to construct the additional Bloch basis for description of the conduction bands were chosen such that the contribution to any overlap matrix element over Bloch orbitals due to the inclusion of the sixth shell of atoms was less than 0.001. Numerical evaluation of the Clebsch-Gordan coefficients incurred was performed to high

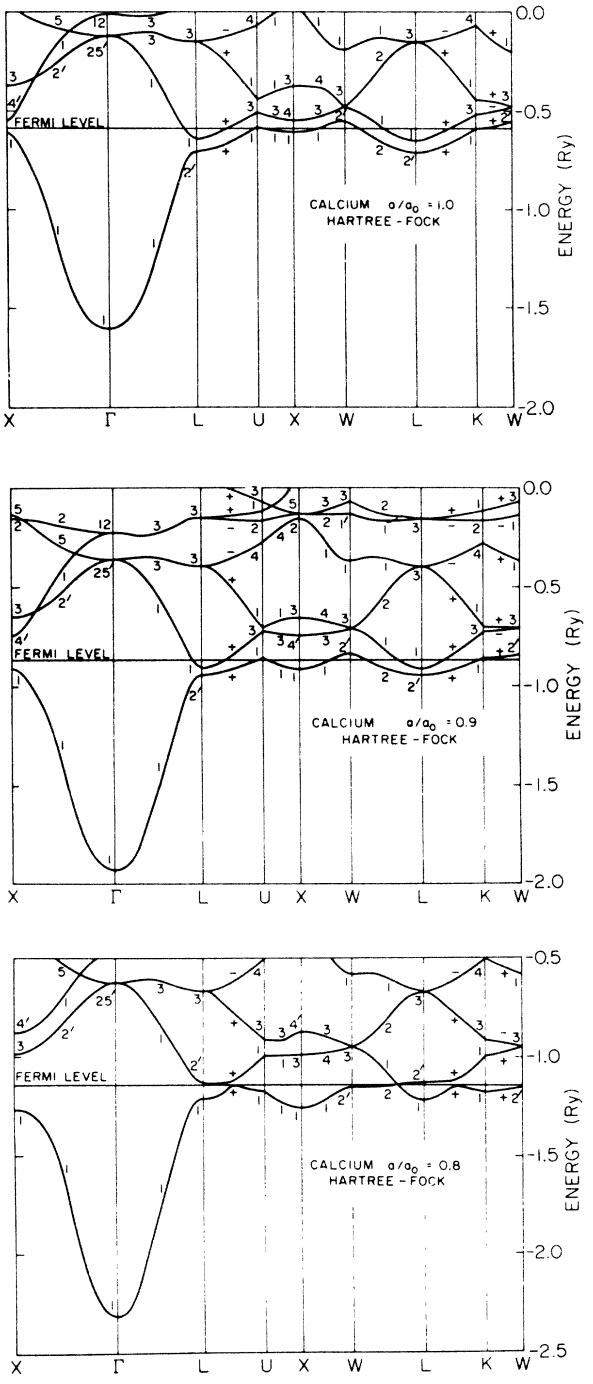

FIG. 1. Band structure of calcium for various lattice constants in the Hartree-Fock approximation ($a_0 = 10.54$ bohr).

precision using a program written by Wills.[38]

The two-step process of first determining the Hartree-Fock orbitals self-consistently within the local orbitals formalism and then performing a final iteration to determine the canonical Hartree-Fock eigenfunctions was performed for lattice spacings a ($a/a_0 = 1.0$, 0.9, 0.8, 0.7). With this information we were able to make extensive comparisons with other calculations and with data from compression experiments. Due to near-linear dependence problems encountered for $a/a_0 = 0.7$, we were not able to obtain accurate bands for all $\vec{k}$ at this lattice spacing. The Hartree-Fock bands for the larger three lattice constants are presented in Fig. 1.

B. Overhauser correlation correction

Having obtained the Hartree-Fock band structure for metallic calcium, we proceeded to include polarization and correlation effects in the calculation. We choose to make these corrections using the model suggested by Lundquist[27] and Overhauser[28] due to its simplicity and its agreement with an earlier study[39] which concentrated on an electron gas in the high-density limit.

The fundamental approximation of the model is the replacement of the complete spectrum of excitation energies by a single-plasmon branch. The formalism is developed by first determining the interaction coefficient M_q for the coupling of a test charge to the plasmon of wave vector $\vec{q}$. The coefficient is determined by requiring fulfillment of the f-sum rule for an electron gas. The interaction Hamiltonian between the test charge at $\vec{r}$ and the plasmon modes is found to be

$$H'(\vec{r}) = \sum_{\vec{q}} M_q (a_{\vec{q}} e^{i\vec{q}\cdot\vec{r}} + a_{\vec{q}}^{\dagger} e^{-i\vec{q}\cdot\vec{r}}) , \tag{4}$$

with

$$M_q = \left(\frac{2\pi e^2 \hbar \omega_p^2}{q^2 \omega_q}\right)^{1/2} \tag{5}$$

and

$$\omega_p^2 = 4\pi N e^2/m\Omega , \tag{6}$$

the square of the classical plasma frequency. The operators $a_{\vec{q}}^{\dagger}$ and $a_{\vec{q}}$ are plasmon creation and annihilation operators, respectively.

The plasmon frequency spectrum

$$\omega_q^2 = \omega_p^2 \epsilon_q/(\epsilon_q - 1) \tag{7}$$

is obtained by equating the electrostatic energy of interaction associated with each Fourier component as determined by classical field theory and that determined by second-order perturbation theory. The dielectric function ϵ_q remains to be determined and is derived using perturbation theory on an electron-gas subject to a self-consistent potential. The change in the exchange and correlation potential due to the perturbation is simply found by assuming the local Kohn-Sham potential.[2] The generalized result is

$$\epsilon_q = 1 + Q(x)/[1 - G(x)Q(x)] , \tag{8}$$

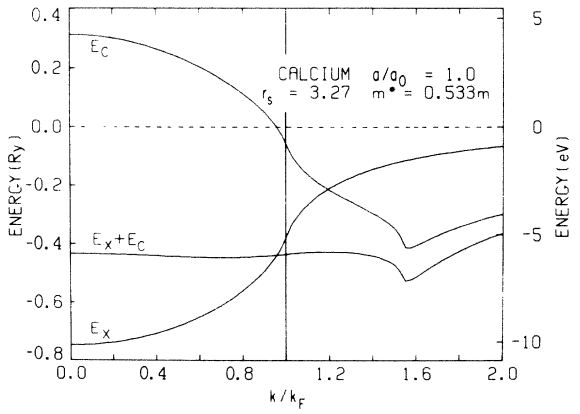

FIG. 2. Exchange energy E_x and correlation energy E_c and their sum for an electron gas with density of calcium and effective mass $m^* = 0.533m$.

with $x = q/2k_F$, $G(x) = x^2 g(x)$, $Q(x) = Cf(x)/x^2$, $C = me^2/\pi\hbar^2 k_F$, and

$$f(x) = \tfrac{1}{2} + [(1-x^2)/4x]\ln\left|(1+x)/(1-x)\right| . \quad (9)$$

The limiting behavior of $g(x)$ is determined by means of arguments involving compressibility relations (for $x \to 0$) and pair correlation functions (for $x \to \infty$). The behavior at intermediate x was determined by requiring the subsequently determined correlation energy to duplicate that calculated by a previous paper.[40] The function adopted for $g(x)$ is

$$g(x) = 1.1/(1 + 10x^2 + 1.5x^4)^{1/2} \quad (10)$$

The equations reviewed so far have described the interaction of a fixed test charge with the plasmons. These equations are then extended to include the exchange and correlation potential associated with an electron. The extension simply requires that the interaction coefficient be replaced by

$$M_q' = M_q[1 - G(x)] . \quad (11)$$

Using second-order perturbation theory, the one-electron correlation energy $E_c(\vec{k})$ is determined by taking the difference between the total system interaction energy with $|\vec{k}\rangle$ occupied and with $|\vec{k}\rangle$ empty:

$$E_c(\vec{k}) = E_c(k) = \sum_{|\vec{k}-\vec{q}|>k_F} \frac{M_q^2[1-G(x)]^2}{E(\vec{k}) - E(\vec{k}-\vec{q}) - \hbar\omega_q} - \sum_{|\vec{k}+\vec{q}|<k_F} \frac{M_q^2[1-G(x)]^2}{E(\vec{k}+\vec{q}) - E(\vec{k}) - \hbar\omega_q} \quad (12)$$

The one-electron energy $E(k)$ for an interacting electron gas is the sum of the three contributions:

$$E(k) = \hbar^2 k^2/2m + E_x(k) + E_c(k) , \quad (13)$$

where the exchange energy $E_x(k)$ has the usual form

$$E_x(\vec{k}) = E_x(k) = -(2e^2 k_F/\pi) f(y) , \quad (14)$$

with $f(y)$ given by Eq. (9) and $y = k/k_F$.

Overhauser shows that the infinite slope at $k = k_F$ appearing in $E_x(k)$ is exactly canceled by a similar property in $E_c(k)$. In addition, he shows that the sum of these two terms is essentially constant for all values of k, and that $E_c(k)$ is relatively small when $k \approx k_F$. This implies that a Hartree-Fock calculation which treats the point-charge lattice correctly will give substantially correct one-electron energies for $k \approx k_F$, since the correlation corrections are minimal there. The most severe drawback of using this model to include correlation corrections to the bands is its $\vec{k}$-direction independence.

Correlation corrections made to the $a/a_0 = 1.0$ Hartree-Fock bands are indicated graphically in Fig. 2 by the curve marked E_c. Also included in Fig. 2 are curves for the free-electron exchange E_x and the sum of these two curves. These curves are analogous to those appearing in Fig. 2 of Ref. 28, but modified for calcium with an equivalent-sphere radius $r_S = 3.27$ and effective mass $m^* = 0.533m$. The effective mass was determined by forcing the valence band width of the free-electron bands (including exchange) to match the width of the Hartree-Fock bands. The purpose in using m^* is to include in an elementary way the effect of the lattice in free-electron bands and the correlation energy.

The relationship between free-electron bands and Hartree-Fock bands ($a/a_0 = 1.0$) with and without correlation corrections is shown in Fig. 3. In panel (A) the free electron bands for an electron gas with the density of calcium and $m^* = 0.533m$ is shown. In panel (B) the exchange energy E_x of Fig. 2 has been added to the free-electron bands, and in panel (C) the correlation energy E_c of Fig. 2 has also been added. Hartree-Fock bands are presented in panel (D), and in panel (E) the correlation energy of Fig. 2 has been added to the Hartree-Fock bands. The effective mass m^* was chosen to force the width of the valence band of panel (B) to match that appearing in panel (D). Panel (C) represents the best calcium bands determined within the free-electron approximation and Overhauser's method of including correlation effects. Panel (E) represents our final Hartree-Fock bands corrected for electron correlation.

In order to determine the correlation correction appropriate for Hartree-Fock Bloch state with energy $E(\vec{k}^{HF})$ and wave vector $\vec{k}^{HF}$ we use the corresponding free-electron-plus-exchange wave-vector magnitude k determined by solving the equation

$$E^{HF}(\vec{k}^{HF}) = E(k) = (\hbar^2/2m^*)k^2 + E_x(k) \quad (15)$$

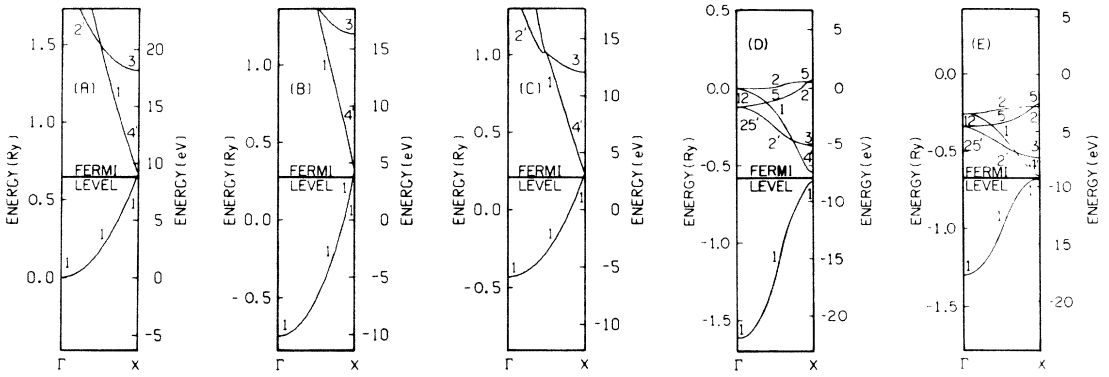

FIG. 3. The relationship between free-electron bands and Hartree-Fock bands ($a/a_0 = 1.0$) with and without correlation corrections. Panel (A): free-electron bands for an electron gas with the density of calcium and $m^* = 0.533m$. Panel (B): free electron bands with exchange energy E_x. Panel (C): free-electron bands with exchange-correlation energy $E_x + E_c$. Panel (D): Hartree-Fock bands. Panel (E): Hartree-Fock bands with correlation energy E_c.

for k. The correlation correction $E_c(k)$ is calculated for this k and added to $E(\vec{k}^{HF})$. The correlation corrected bands for lattice spacings a ($a/a_0 = 1.0$, 0.9, and 0.8) are presented in Fig. 4.

In Fig. 5 we present for comparison, using the same scale, augmented-plane-wave (APW) bands for the equilibrium lattice spacing $a/a_0 = 1.0$ obtained by McCaffrey, Anderson, and Papaconstantopoulos.[41] The Kohn-Sham[2] ($\alpha = \frac{2}{3}$) local exchange was used. The band energies (Ry) at points of high symmetry for calcium for $a/a_0 = 1.0$ are listed in Table II. Three cases are included: Hartree-Fock, Hartree-Fock with electron correlation corrections, and APW with a local exchange approximation ($\alpha = \frac{2}{3}$).[41]

C. Density of states

The bands are calculated at 89 uniformly distributed points $\vec{k}_i$ within the irreducible wedge of the Brillouin zone. The density of states is calculated using the Lehmann and Taut[42] adaption of the Gilat and Raubenheimer[43] "linear analytic" (LA) method. Instead of the discrete nature of sampling that is usually employed in other methods,[44] analytical or continuous integration is performed throughout small tetrahedra whose vertices are defined by the points $\vec{k}_i$. The integration is accomplished by calculating numerically the area of a constant-energy plane surface that lies within each tetrahedron.

A recent analysis of methods for calculating spectral properties of solids has been made by Gilat[44] who finds: "Generally, the LA method is to be preferred in all cases where either high resolution and accuracy are desired or computational speed is needed, or both."

We express the density of states $N(E)$ in units of states $\mathrm{Ry}^{-1}\mathrm{atom}^{-1}$ and have multiplied by 2 in order to take spin into consideration:

$$N(E) = \frac{2v_c}{(2\pi)^3} \sum_i \oint \frac{dS}{|\vec{\nabla}_{\vec{k}} E_i(\vec{k})|} \tag{16}$$

where v_c is the volume of the Wigner-Seitz cell. One need only integrate the density of states of the valence band over energy until the area equals 2 (in the case of divalent materials such as calcium) to find the Fermi level E_F. Due to the unique manner of obtaining self-consistency, the matching of hole states in the first zone with the electron states in the second zone is exact. The electronic specific heat $C_e = \gamma T$ is determined by the density of states at E_F by means of the equation[45]

$$\gamma = \tfrac{1}{3}\pi^2 N(E_F) k_B^2 \tag{17}$$

or

$$\gamma\left[\frac{\mathrm{mJ}}{\mathrm{mole}\ ^\circ\mathrm{K}^2}\right] = 0.17322 N(E_F)\left[\frac{\mathrm{states}}{\mathrm{Ry\ atom}}\right]. \tag{18}$$

Densities of states for the valence and conduction bands of calcium in the Hartree-Fock approximation for lattice spacings a ($a/a_0 = 1.0$, 0.9, and 0.8) are presented in Fig. 6. The densities of states corrected for electron correlation and for the same lattice spacings are presented in Fig. 7. In Fig. 8 we reproduce for comparison the density of states derived from the APW–local-exchange calculation.[41]

D. Zero density of states at Fermi level

There is an interesting result[46] associated with the theory of a free-electron gas which is frequently referred to when discussing the inadequacies of the Hartree-Fock approximation. It is the rapid falloff to zero of the density of states as the Fermi level is approached. Zero density of states implies zero specific heat. Since this is not observed experimentally the conclusion is that the Hartree-Fock theory possesses serious inadequa-

TABLE II. The energies (Ry) at points of high symmetry for calcium for $a/a_0 = 1.0$. Also included are the density of states at the Fermi surface $N(E_F)$ [states Ry^{-1} $atom^{-1}$] and the constant γ [$mJ\,°K^{-2}\,mole^{-1}$] entering the specific-heat expression. Column under "HF" gives Hartree-Fock results, "HF + E_c" gives Hartree-Fock results corrected for electron correlation by Overhauser's method and "Local E_x" gives the results obtained from an APW calculation using the Kohn-Sham local exchange approximation (Ref. 41).

	HF	HF + E_c	Local E_x
Γ_1	−1.6071	−1.2949	0.0290
Γ'_{25}	−0.1223	−0.3484	0.5590
Γ_{12}	−0.0131	−0.2578	0.6530
X_1	−0.6133	−0.6815	0.2902
X'_4	−0.5469	−0.6578	0.4020
X_3	−0.3728	−0.5455	0.4023
L'_2	−0.7084	−0.7106	0.3068
L_1	−0.6493	−0.6835	0.2643
L_3	−0.1526	−0.3742	0.7220
W'_2	−0.5503	−0.6601	0.3392
W_3	−0.4786	−0.6185	0.3977
W_1	−0.1989	−0.4114	0.5407
K_1	−0.5867	−0.6761	0.3265
K_3	−0.5116	−0.6384	0.4006
K_1	−0.4477	−0.5990	0.3788
K_4	−0.0708	−0.3054	0.6250
E_F	−0.587	−0.6750	0.3250
$N(E_F)$	4.19	14.19	11.20
γ	.73	2.46	1.94

cies.

There is a general argument[47] supporting the concept of finite energy differences between adjacent occupied and unoccupied levels and consequently a zero density of states at the Fermi level. It is that an electron in an occupied level is acted upon by an effective $N-1$ electron charge density, whereas an electron in a virtual orbital is acted upon by an N electron charge density. This occurs because the exchange term in the Hartree-Fock operator serves to effectively remove an electron from the total charge distribution acting on an occupied state as a means of preventing terms involving the self-interaction from being included in the energy expression. Although the electronic charge removed is just one in 10^{23}, is is localized about the electron in the occupied state (the removed charge constitutes a "Fermi hole"). The degree of interaction of this "hole" with the electron and environment and consequently the localized nature of the "hole" determines the size of the energy difference between the occupied and unoccupied levels. If the Fermi hole is completely delocalized, then the energy of interaction would simply be equal to the energy difference associated with environments composed of N and $N-1$ electrons, which is of the order of $e^2/\Omega^{1/3} \approx 10^{-7}$ eV for $\Omega \approx 1$ cm^3. The hole is known to be nonspherical

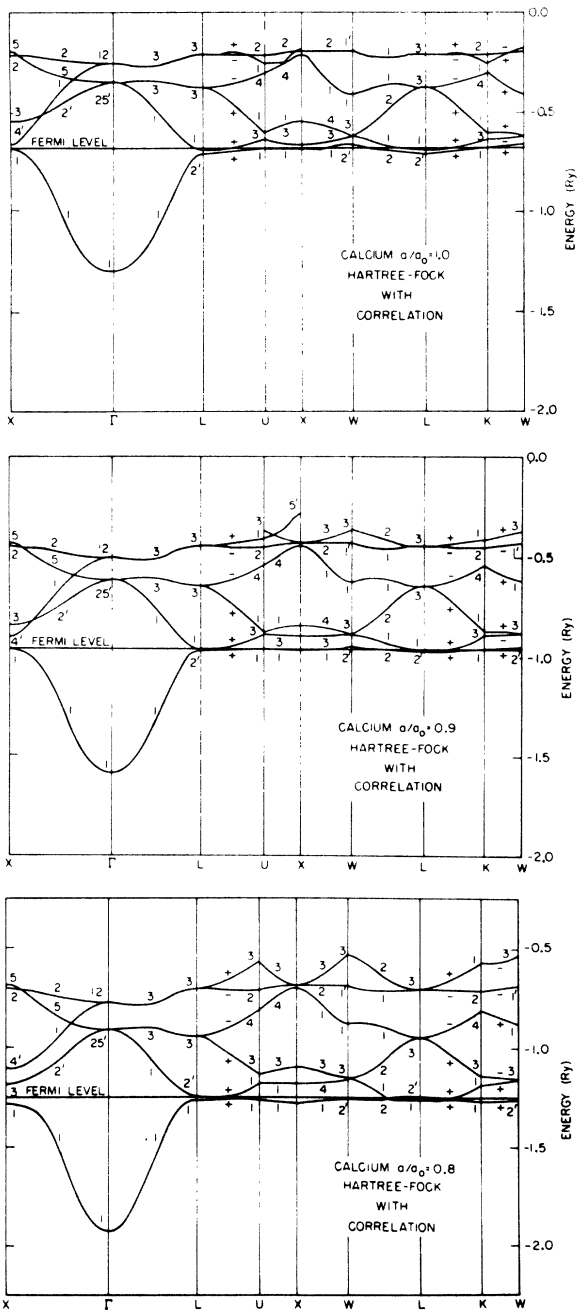

FIG. 4. Band structure of calcium for various lattice constants a in the Hartree-Fock approximation corrected for electron correlation effects.

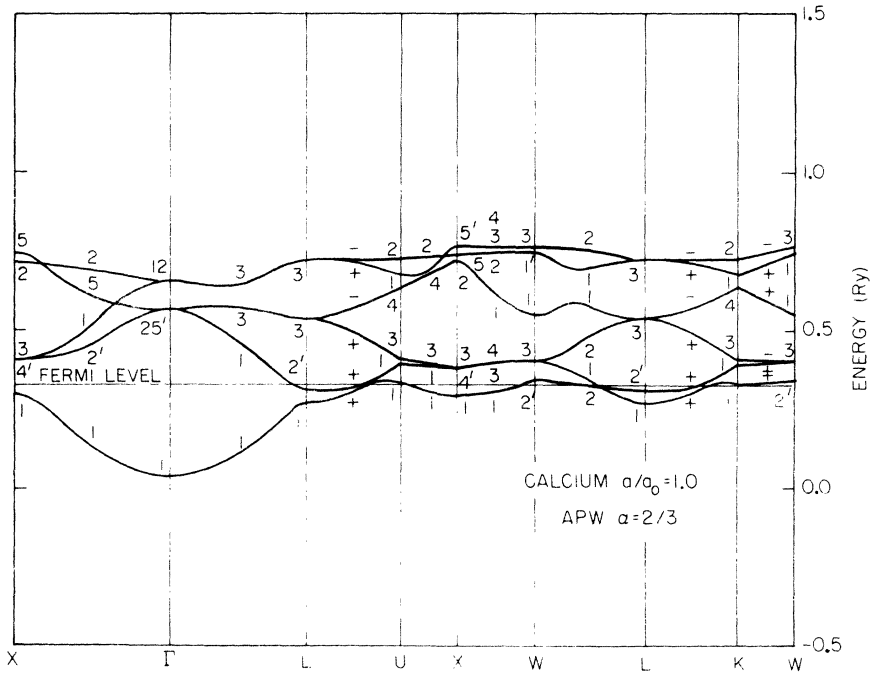

FIG. 5. Band structure of calcium for equilibrium lattice constant a_0 obtained by McCaffrey, Anderson, and Papaconstantopoulos (Ref. 41) using the APW method and the Kohn-Sham ($\alpha = 2/3$) local exchange approximation.

and described by means of a complex distribution function. We maintain that it is not possible, *a priori*, to determine the degree of localization of the Fermi hole in a real crystal due to its involved nature and, therefore, that it is not justifiable to assume that the density of states will necessarily approach zero at the Fermi level with a strength that can be described by any band-calculation method for real crystals now in existence. Indeed, our calculations do not reveal[48] the tendency of the density of states to fall to zero as the Fermi level is approached.

E. Joint density of states and ϵ_2

We have used the LA $\vec{k}$-space integration as suggested by Lehmann and Taut[42] to evaluate the joint density of states and the imaginary part ϵ_2 of the complex dielectric function. The joint density of states is expressed as

$$N_J(E) = \frac{2v_c}{(2\pi)^3} \sum_{i,j} \oint_{E_i - E_j = E} \frac{dS}{|\vec{\nabla}_{\vec{k}}[E_j(\vec{k}) - E_i(\vec{k})]|} \,. \tag{19}$$

Since we are concerned only with optical excitations from the flat 1s band to the conduction band, the joint density has the identical shape of the conduction-band density of states.

The expression for ϵ_2 is due to Ehrenreich and Cohen[49] and is given by

$$E\epsilon_2(E) = \frac{e^2\hbar^2}{2\pi m} \sum_{i,j} \oint_{E = E_i - E_j} \frac{f_{ij}(\vec{k})\, dS}{|\vec{\nabla}_{\vec{k}}[E_j(\vec{k}) - E_i(\vec{k})]|} \,, \tag{20}$$

where the oscillator strengths are given by

$$f_{ij}(\vec{k}) = \frac{2}{3m} \frac{|\langle \vec{k}, i | \vec{p} | \vec{k}, j \rangle|^2}{E_j(\vec{k}) - E_i(\vec{k})} \,, \tag{21}$$

with $\vec{p} = (\hbar/i)\vec{\nabla}$. The evaluation of the oscillator strengths is approximately as time consuming as the evaluation of the Hartree-Fock eigenfunctions. The number of matrix elements and rotation coefficients is larger, since the momentum operator is composed of three parts and must be rotated along with the spherical harmonics on which it acts. The momentum operator is replaced by the corresponding irreducible tensor operator of rank 1 in order to maintain real matrix elements. Blume and Watson[50] give all necessary expressions which occur when the tensor operator acts on spherical harmonics.

In order to make a meaningful interpretation of the 1s emission and absorption data available for calcium, we have calculated the imaginary part of the complex dielectric constant ϵ_2 according to Eqs. (20) and (21). The results are given in Fig. 9 for the correlated bands at the equilibrium lattice spacing. No correlation corrections have been calculated for the inner electrons or the electron-hole interaction.[51] However, the scale has been shifted downward 28.6 eV so that the experimental Fermi level is reproduced at 4036.4 eV. It should be pointed out that the original Hartree-Fock eigenfunctions have been used in the calculation of the momentum matrix elements. The only way in which the correlation corrections and the shift in scale affects the evaluation of ϵ_2 is through the energy terms in the divisor. This approximation is

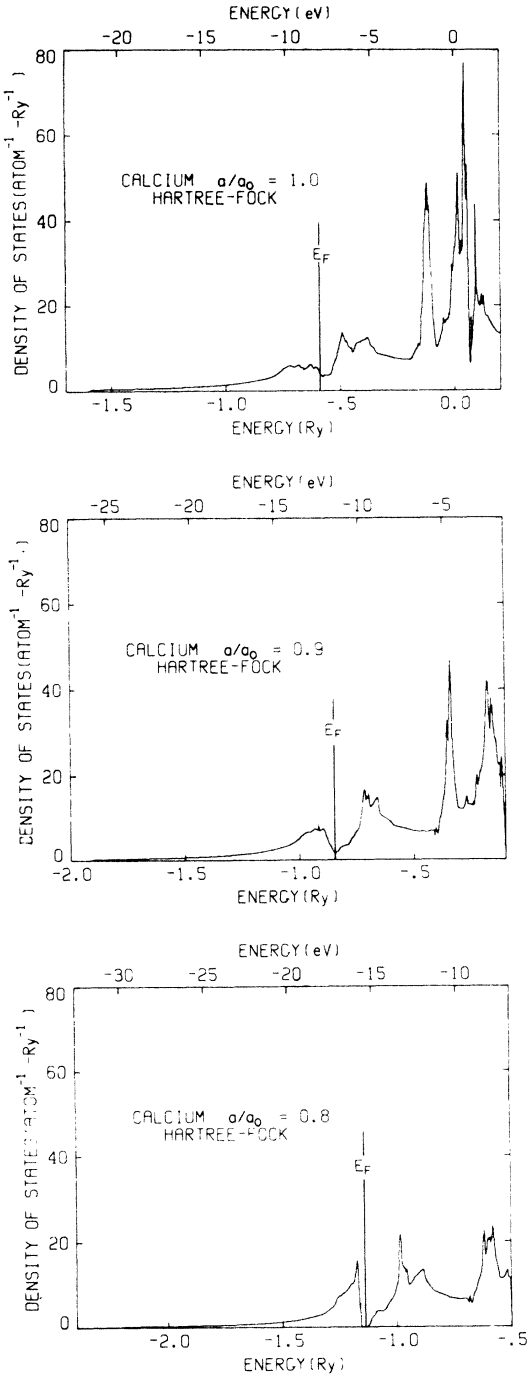

FIG. 6. Density of states of valence and conduction bands derived from the Hartree-Fock bands.

quite reasonable especially when it is realized that in most studies the momentum matrix elements are assumed constant. The oscillator strength for direct calcium 1s transitions used in the calculation of ϵ_2 is given in Fig. 10. The experimental 1s absorption and emission data are reproduced in Fig. 11 from the work of Finkelshteyn and Nemnonov.[52] The broken line represents the calcium emission curve after corrections are made for the presence of CaO. The Fermi level is found from the intersection of the emission and absorption bands.

F. Fermi surface

The description of the shape of the Fermi surface has been one of the most difficult challenges of theoretical calculations on metals. Our attempt to predict de Haas–van Alphen orbit areas are summarized in Table III. We give results for both the uncorrelated and correlated Hartree-Fock bands. Also presented are the recent experimental results obtained by Jenkins and Datars[53] and the results obtained from an APW ($\alpha = \frac{2}{3}$) calculation.[41] Percentage errors of the theoretical results from the experimental results are given in parentheses. In Fig. 12 we present the de Haas–van Alphen orbits corresponding to those listed in Table III. The solid lines indicate orbits obtained from uncorrelated Hartree-Fock bands and the broken lines indicate orbits obtained from correlated Hartree-Fock bands.

III. DISCUSSION

A. Pressure-induced electronic transitions

One of the most interesting properties of calcium is its high-pressure-induced anomalies in electrical conductivity. Suggestions that these anomalies exist were first made by Altmann and Cracknell.[54] Almost simultaneously Stager and Drickamer[55] experimentally confirmed the predictions. The experimental resistance versus pressure results[56] are summarized in Fig. 13 for two temperatures. There is an increase in resistance with increasing temperature, as expected for a metal, at all pressures except in the region 300–400 kbar. In this region calcium acts as a semiconductor with respect to its temperature dependence on resistance. The phenomenon has been at least qualitatively explained by most calculations on calcium as being due to metal-to-semimetal-to-metal electronic transitions caused by increasing pressure. We refer the reader to the recent paper by McCaffrey, Anderson, and Papaconstantopoulos[41] for a review of both the experimental and theoretical works on calcium. We will use their work as a standard of previous work.

Both the Hartree-Fock bands (Fig. 1) and the Hartree-Fock bands with correlation corrections (Fig. 4) support the metal-to-semimetal-to-metal electronic transition explanation of the resistance anomaly. For $a/a_0 = 1.0$ the Fermi surface cuts the bands in such a way that there is a significant density of states both above and below the Fermi level (Figs. 6 and 7). Calcium is therefore predicted to behave as a metal at equilibrium lattice

spacing. The 4s and 3d atomic levels merge to form a partially filled band that possesses essentially the same structure (except for valence band width) as in previous studies. It should be noted that, in contradiction with most earlier studies as in Fig. 5, the bands from the first and second

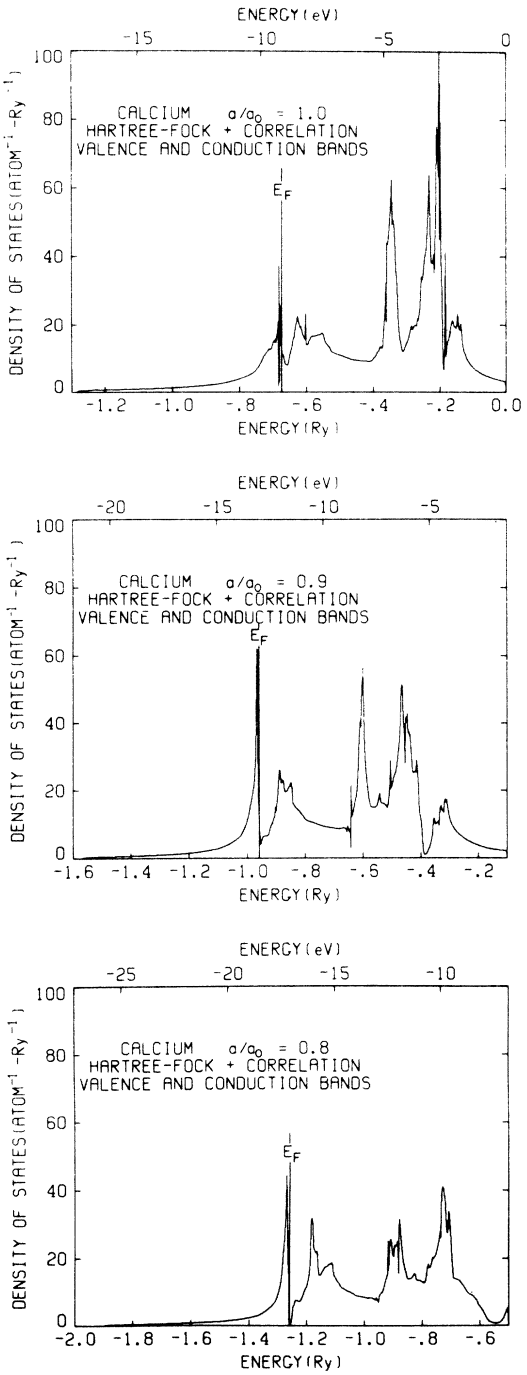

FIG. 7. Density of states of valence and conduction bands derived from the Hartree-Fock results corrected for electron correlation.

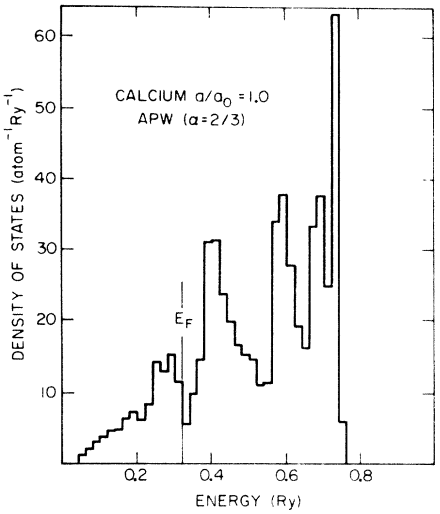

FIG. 8. Density of states of calcium for equilibrium lattice constant a_0 obtained using the APW method and a local exchange approximation (Ref. 41).

Brillouin zones do not cross near the Fermi level. In fact, for the uncorrelated Hartree-Fock case, these bands show an unusual parallelism near the zone boundary.

When the lattice spacing is reduced to $a/a_0 = 0.9$, the parallelism in the Hartree-Fock bands (Fig. 1) is removed by the converging of the bands at L_1 and L_2' near the Fermi level. Figure 4 shows the Hartree-Fock bands after correlation corrections have been made. The density of states surrounding the Fermi level has diminished greatly in both cases (Figs. 6 and 7).

The metal-to-semimetal electronic transition is predicted to be complete at a lattice spacing of

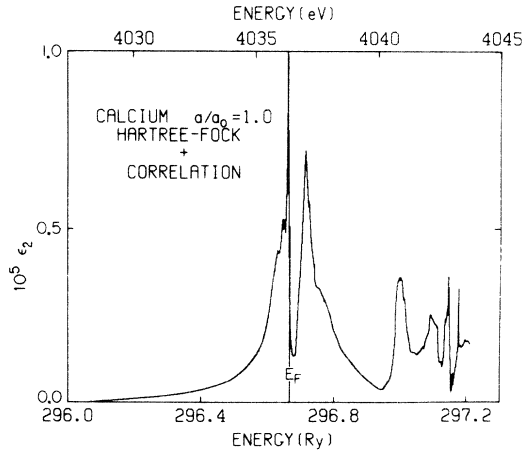

FIG. 9. Imaginary part ϵ_2 of the complex dielectric function for direct calcium 1s transitions. Correlation corrections for valence and conduction electrons have been made by Overhauser's method. The scale has been shifted so that experimental Fermi level is matched.

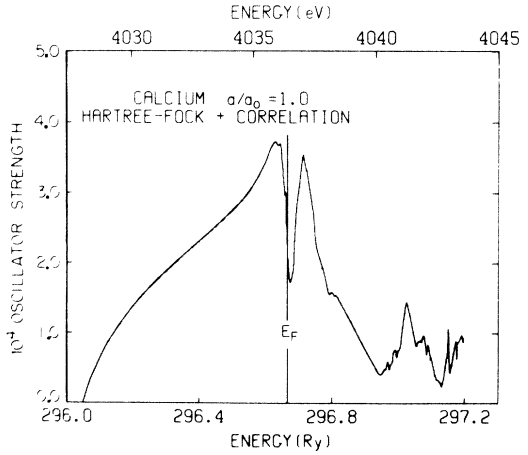

FIG. 10. Oscillator strength for direct calcium 1s transitions. Correlation corrections for valence and conduction electrons have been made by Overhauser's method. The scale has been shifted so that the experimental Fermi level is matched.

$a/a_0 = 0.8$. In both the uncorrelated and correlated Hartree-Fock cases, the Fermi level cuts the bands at only a single point in the irreducible wedge. The density of states is accordingly infinitely small at the Fermi level. At this lattice spacing the bands from the first and second Brillouin zones have converged and crossed along the direction W-L. The surfaces of the two zones make contact at only this single point in the irreducible wedge and consequently the Fermi surface must pass through this point in order to match the electrons in the second zone with the number of holes in the first.

It is interesting to note that the uncorrelated and correlated Hartree-Fock density of states for $a/a_0 = 0.8$ shows a definite range of energies (0.2 eV) for which the density is negligibly small. So, at a reduced lattice spacing of $a/a_0 = 0.8$, calcium possesses both the property of being a metal (the Fermi surface cuts the bands) and the property of a semiconductor (the existence of a "band gap" of 0.2 eV in the density of states about the Fermi level). The term "semimetal" is therefore appropriately applied to calcium at this lattice spacing. We find that our Hartree-Fock calculation correctly predicts semiconductor-like dependence or resistance on temperature at high pressures.

Although we were unable to obtain accurate bands for all $\vec{k}$ with a lattice spacing of $a/a_0 = 0.7$, the trends indicate that the bands at X_3 will continue to drop sufficiently so that X_3 will lie below the Fermi level and the bands near the point of crossing along W-L will rise above the Fermi level. Since the Fermi surface will cut the bands at a large number of points, there will be a significant density of states surrounding the Fermi level and calcium will return to a metal.

The lattice spacings at which the electronic transitions occur can be interpolated from a plot of the correlated Hartree-Fock energies X_3, W_2', L_2', and E_F as a function of a/a_0 as in Fig. 14. The metal-to-semimetal transition occurs at approximately $a/a_0 = 0.82$ when L_2' and W_2' converge to the same energy (E_F). The semimetal-to-metal transition at approximately $a/a_0 = 0.7$ may not be accurate due to linear-dependence problems mentioned earlier.

The first transition at $a/a_0 = 0.82$ can be compared with the APW value[41] of 0.93 and the "experimental" value of 0.875 determined by Altmann, Harford, and Blake[57] using an equation of state. Our value of $a/a_0 = 0.725$ for the second transition can be compared with the APW value of 0.8. The correlated Hartree-Fock bands predict electronic transitions at smaller lattice spacings than does the APW bands, but both are in about 6% error with the "experimental" value.

B. Optical properties

The optical spectra of crystalline solids are primarily dependent on the density of states of the bands involved in the transition. In some regions of the spectra transition, matrix elements can and do significantly enhance or depress peaks in the density of states and therefore cannot be ignored when calculating emission and absorption spectra. We rigorously include dipole transition

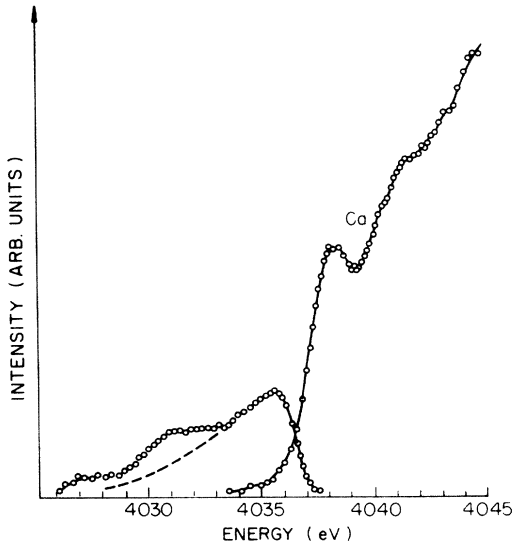

FIG. 11. K emission band (broken line) after elimination of the effects due to CaO contamination. K absorption band is shown at right. Intersection locates Fermi level. Vertical axis indicates absorption in arbitrary units. Reproduced from Ref. 52.

TABLE III. Experimental and theoretical de Haas–van Alphen data for $a/a_0 = 1.0$. Experimental results are from Jenkins and Datars (Ref. 53). Theoretical results are from our Hartree-Fock (HF), Hartree-Fock with correlation corrections (HF + E_c) and from the McCaffrey, Anderson, and Papaconstantopoulos augmented-plane-wave (APW) (Ref. 41) calculations. Percentage errors from experiment are given in parentheses.

		Experiment			HF	HF + E_c	APW ($\alpha = 2/3$)
Orbit	$\vec{B}$	P (10^{-7} G^{-1})	ν[10^4 G]	$A[(2\pi/a)^2]$	$A[(2\pi/a)^2]$	$A[(2\pi/a)^2]$	$A[(2\pi/a)^2]$
α	[100]	0.7843	1275	0.09584	0.043 (55%)	0.049 (49%)	0.12 (25%)
β	[110]	0.5814	1720	0.1293	0.10 (23%)	0.10 (23%)	0.05 (61%)
γ	[110]	3.077	325	0.12443	0.0032 (97%)	0.0 (100%)	0.009 (93%)
δ	[110]	0.7874	1270	0.09546	0.089 (6.8%)	0.093 (2.6%)	0.15 (57%)

matrix elements in our calculation of ϵ_2, the imaginary part of the complex dielectric function.

The experimental results (Fig. 11) show a 1s-valence emission band having a width exceeding 7 eV. The experimental 2p-valence emission band[58] is essentially identical in every respect. A 3p-valence emission band spectrum obtained by Kingston,[59] however, has a width of 3 eV. Since the 1s band is flat, the emission band width must be due to the valence band width, assuming electron-hole interactions and local field effects are negligible.[60] The Hartree-Fock valence band width for $a/a_0 = 1.0$ (Fig. 1) exceeds 13 eV and thus is greater than experiment. This is consistent with the results obtained in the cases of the alkali halides,[15] the rare gas solids,[15,16] and beryllium.[17] However, when electron correlation corrections are made, good agreement with experiment is obtained.[15] This is also true in the case of calcium since the *correlated* Hartree-Fock bands for $a/a_0 = 1.0$ (Fig. 4) show a valence band width of approximately 8 eV. This compares favorably with two[52,58] of the three existing experimental emission curves especially when one considers the extent of the low-energy tails on both the experimental data and on the calculation of ϵ_2 (Fig. 9). It is interesting to note that essentially all calculations employing a local exchange approximation (see, e.g., Fig. 5) yield a valence band width of about 3 eV which compares favorably with the one[59] remaining experimental result.

The shape of the valence-1s emission spectra as predicted by our calculated ϵ_2 curve is somewhat different than that experimentally observed. The peak just below the Fermi level is very close to the Fermi level and the tail toward lower energies is more skewed. The effect of the oscillator strength (Fig. 10) when included with the density of states (Fig. 7) to form ϵ_2 is seen to be a gradual, almost linear, enhancement of the spectrum from the low energy onset to within 0.5 eV of the Fermi level. From that point to the Fermi level, the oscillator strength falls abruptly. Although the transitions involved are from a 1s band to an s- and/or d-like valence band, and the atomic selection rules would predict zero oscillator strength, there are a significant number of points in $\vec{k}$ space away from Γ which do allow nonzero oscillator strengths.

Our agreement with the experimental absorption data is less apparent. However, there is a remarkable agreement for energies above the Fermi level between the correlated Hartree-Fock density of states (Fig. 7), that obtained from an APW calculation with a local exchange approximation (Fig. 8), and a recent Korringa-Kohn-Rostoker (KKR) calculation[61] also employing a local exchange approximation. The only significant differences are a smaller peak just above E_F and a greater distance between peaks of about 12% in the correlated Hartree-Fock case.

The calculation of ϵ_2 does not show the broad band exhibited in the experimental absorption spectrum. The oscillator strengths for this region of the spectrum are rather small and depress the peaks present in the density of states. There are two structures on the broad band, lying at about 4038.3 and 4041.7 eV. We associate the first and second peaks seen in our calculation of ϵ_2 with these structures since the absolute positions of the peaks are correct within 2 eV and the distance between them is correct within 0.5 eV.

There appear to be two possible interpretations of the origin of the broad band. The first is that our inclusion of only dipole matrix elements is a poor approximation, since large photon energies are involved and the approximation $e^{i\vec{k}\cdot\vec{r}} \rightarrow e^{ika} \approx 1$ is not true (a is the radius of final 1-el charge density; $\vec{k}$ is the wavevector of photon). The transitions involved are from s to s bands or s to d bands and therefore have small dipole oscillator strength. Higher multipole transitions may be of considerable importance. The second interpretation of the origin of the broad band is simply that it is due to multiple band-to-band excitations, collective phonon excitations, or electron-hole interactions.

It is interesting to note a very recent study of the 1s absorption spectrum by McCaffrey and Papa-

constantopoulos[62] using their computed APW bands; the bands we have been using as a standard. Although their density of states agrees remarkably well with ours, the oscillator strength and optical-absorption spectrum significantly differ from ours.

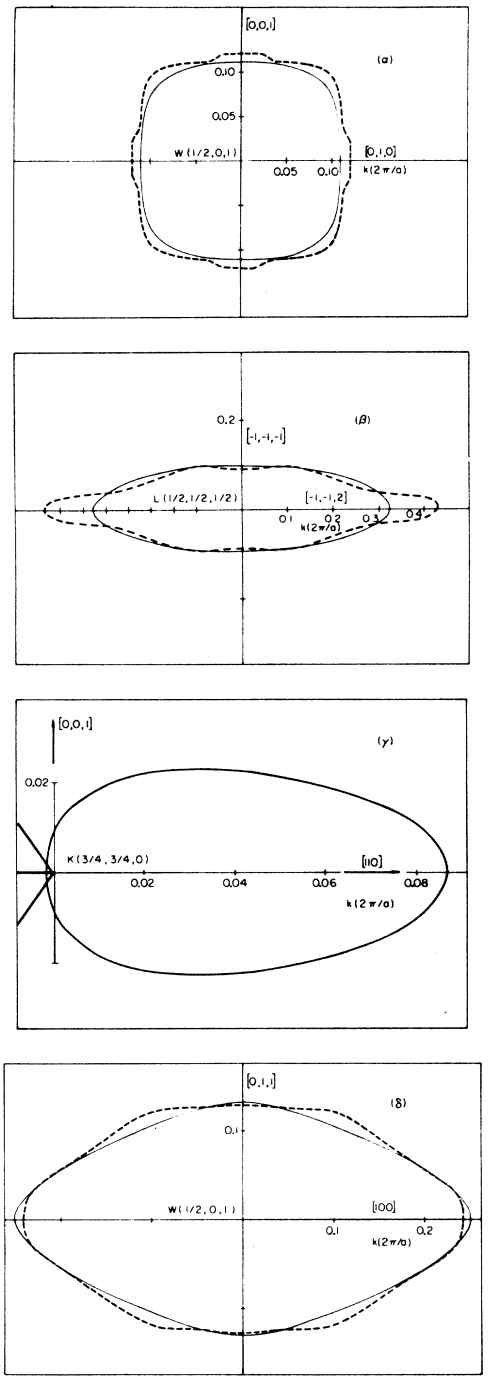

FIG. 12. de Haas–van Alphen α, β, γ, δ orbits of calcium for $a/a_0 = 1.0$. Solid lines indicate orbits obtained from Hartree-Fock bands; broken lines indicate orbits obtained from correlation corrected Hartree-Fock bands.

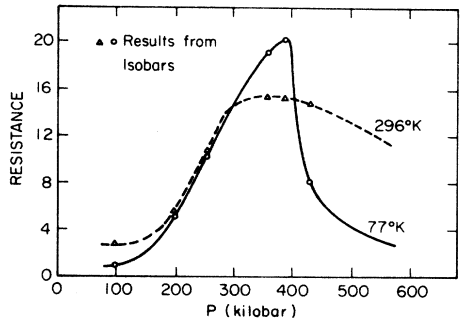

FIG. 13. Resistance versus pressure for calcium. Reproduced from Ref. 56.

This is probably due almost exclusively to the manner in which the dipole matrix elements are approximated in the APW case. The elements were determined by evaluating the matrix elements of the position vector $\vec{r}$ rather than the matrix element of the gradient operator $\vec{\nabla}$. This would not normally have been an approximation except that the 1s Bloch eigenfunction was replaced by a 1s atomic orbital. The approximations also included integration only within the APW sphere.

The APW oscillator strength was found to be a very smooth function of energy and monatonically increasing in contrast with our results shown in Fig. 10. Notwithstanding the approximations, the APW was found to match experiment much better

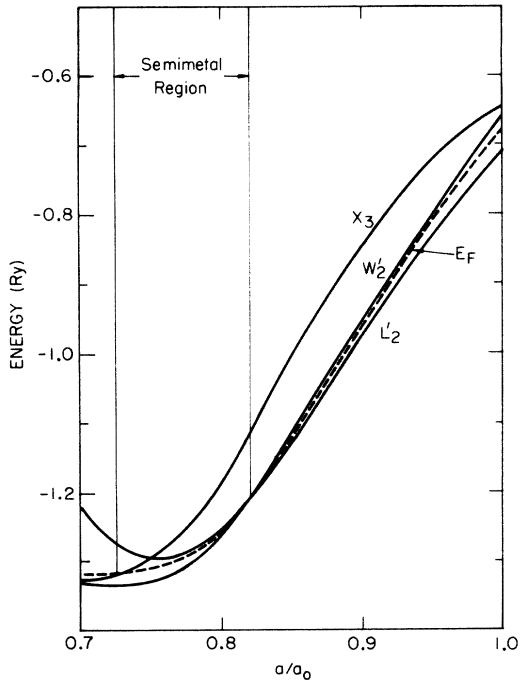

FIG. 14. Variation with lattice spacing of correlated Hartree-Fock energy bands at selected symmetry points.

than the present case in that the broad band on the high-energy side was obtained.

C. Fermi surface

Since the correlation corrections determined by means of Overhauser's simplified method are small for electrons near the Fermi energy, there is little difference in the predicted de Haas–van Alphen orbit areas between the results predicted by the uncorrelated and the correlated Hartree-Fock bands (Table III and Fig. 12). Our results are no better than those obtained by means of the method employing local exchange approximations (see Table III), and so our Hartree-Fock calculations have failed in an area where accurate results have consistently remained elusive. The experimental data suggests that the Fermi surface in the first Brillouin zone is made up of interconnecting arms.[63] The Hartree-Fock results predict a connected Fermi surface, but the cross section at the point of connection (area of orbit γ) is 97% too small. Making correlation corrections only serves to disconnect the Fermi surface (area of orbit γ becomes zero).

Our prediction of the constant γ [Eq. (17)] appearing in the specific-heat expression also has an error comparable to those obtained by means of local exchange approximations. As given in Table II we obtain a value of $\gamma = 0.73$ (mJ $^\circ$K^{-2} mole^{-1}) for the Hartree-Fock case and $\gamma = 2.46$ (mJ $^\circ$K^{-2} mole^{-1}) for the correlated Hartree-Fock case. These values can be compared with the experimentally obtained value of 2.9 (mJ $^\circ$K^{-2} mole^{-1})[64] after inclusion of an enhancement factor[65] of 1.28 due to electron-phonon interactions. Our estimates of γ then become 0.93 and 3.15, respectively, with errors of 68% and 9%. We see in calculating this physical constant that the small correlation correction to electrons near the Fermi surface is significant.

It should be noted that the calculation of de Haas–van Alphen areas for calcium is very sensitive to the position of the Fermi level due to the flatness of the bands there. Although no qualitative estimates have been made, we observe that a slight lowering of the Fermi level (which was determined[42] with an error of 1%) would improve the predicted areas of orbits α, γ and δ due to the resulting increase in size of those areas. However, the resulting area of the orbit β would be reduced and the resulting value for the constant γ appearing in the specific-heat expression would be increased, both changes being in a direction opposite to that required for improvement. Obviously, the positioning of the Fermi level is not the sole contribution to the errors contained in our calculated de Haas–van Alphen data. Approximations such as the $\vec{k}$-independent electron-correlation corrections must surely make non-negligible contributions.

V. CONCLUSIONS

In this paper we have obtained an *ab initio* band structure for calcium in the self-consistent Hartree-Fock approximation. Correlation corrections are made by means of Overhauser's simplified method. This method of calculation produces good results from an experimental point of view and employs no adjustable parameters. We are able to observe the metal-to-semimetal-to-metal electronic transition with increasing pressure, match the valence band width with the experimental emission spectra, and make preliminary identification of structures observed in the absorption spectra by means of a rigorous calculation of ϵ_2. The details of the Fermi surface as indicated by de Haas–van Alphen data have remained elusive—we predict areas which have large percentage errors when compared to experiment.

We finally conclude that *ab initio* methods are a practical way of studying band structures in general. We are able to compute the bands at a large number of points in the Brillouin zone due to the efficiencies of local orbital and LCAO methods.

ACKNOWLEDGMENTS

The authors wish to express their appreciation to Professor H. G. Drickamer, Professor B. Sonntag, Professor J. Dow, Professor F. C. Brown and Dr. D. L. Wilhite and Dr. D. F. Scofield for their useful discussions and criticisms relating to both the experimental and theoretical questions raised during the course of this study. We also express our appreciation to the staff of the MRL Xerox Σ-5 computing center and to R. F. Illyes, in particular, for their assistance. Finally, we wish to thank Dr. R. N. Euwema for his continued encouragement and Professor R. J. Maurer for his firm support of this research project.

---

*Work supported in part by the Army Research Office under Contract No. DA-HCO4 69 C0007, by the National Science Foundation under Grant No. GH-33634 and by the Aerospace Research Laboratory, Air Force Systems Command, USAF, Wright-Patterson AFB, Ohio, Contract No. F33615-72-C-1506.

†Present address: Photo Products Department, Experimental Station Laboratory, E. I. du Pont de Nemours and Co., Wilmington, Del. 19898.

‡Present address: Department of Applied Physics, Stanford University, Stanford, Calif. 94305.

[1] P. Hohenberg and W. Kohn, Phys. Rev. 136, B864

(1964).
[2]W. Kohn and L. J. Sham, Phys. Rev. 140, A1133 (1965).
[3]T. L. Gilbert (unpublished).
[4]R. Gaspar, Acta Phys. 3, 263 (1954).
[5]J. C. Slater, Phys. Rev. 81, 385 (1951).
[6]J. C. Slater, in *Computational Methods in Band Theory*, edited by P. Marcus, J. Janak, and A. Williams (Plenum, New York, 1971), p. 447.
[7]W. H. Adams, J. Chem. Phys. 34, 89 (1961).
[8]W. H. Adams, J. Chem. Phys. 37, 2009 (1962).
[9]T. L. Gilbert, *Molecular Orbitals in Chemistry, Physics and Biology*, edited by P. O. Lowdin and B. Pullman (Academic, New York, 1964), p. 405.
[10]T. L. Gilbert, *Sigma Molecular Orbital Theory*, edited by O. Sinanoglu and K. B. Wiberg (Yale U. P., New Haven, Conn., 1970), p. 249.
[11]P. W. Anderson, Phys. Rev. Lett. 21, 13 (1968).
[12]P. W. Anderson, Phys. Rev. 181, 25 (1969).
[13]A. B. Kunz, Phys. Status Solidi 36, 301 (1969).
[14]A. B. Kunz, Phys. Rev. B 8, 1690 (1973).
[15]D. J. Mickish and A. B. Kunz, J. Phys. C 6, 1723 (1973).
[16]A. B. Kunz and D. J. Mickish, Phys. Rev. B 8, 779 (1973).
[17]D. G. Shankland, Bul. Am. Phys. Soc. 11, 387 (1966).
[18]F. E. Harris, L. K. Kumar, and H. J. Monkhorst, Phys. Rev. B 7, 2850 (1973).
[19]L. Dagens and F. Perrot, Phys. Rev. B 8, 1281 (1973).
[20]N. O. Lipari and W. B. Fowler, Phys. Rev. B 2, 3354 (1970).
[21]L. Dagens and F. Perrot, Phys. Rev. B 5, 641 (1972).
[22]R. N. Euwema, D. L. Wilhite, and G. T. Surratt, Phys. Rev. B 7, 818 (1973).
[23]A. B. Kunz, Phys. Rev. B 6, 606 (1972).
[24]Y. Toyozawa, Prog. Theor. Phys. 12, 421 (1954).
[25]N. F. Mott and M. J. Littleton, Trans. Faraday Soc. 34, 485 (1938).
[26]W. B. Fowler, Phys. Rev. 151, 657 (1966).
[27]B. I. Lundquist, Phys. Kondens. Mater. 6, 193 (1967).
[28]A. W. Overhauser, Phys. Rev. B 3, 1888 (1971).
[29]T. L. Gilbert, Phys. Rev. A 6, 580 (1972).
[30]See articles in *Advances in Chemical Physics*, edited by R. Lefebvre and C. Moser (Interscience, New York, 1969), Vol. XIV.
[31]D. A. Liberman, Phys. Rev. 171, 1 (1968).
[32]T. C. Collins, R. N. Euwema, D. J. Stuckel, and G. G. Wepfer, Int. J. Quantum Chem. S4, 77 (1971).
[33]A. B. Kunz, Phys. Rev. B 7, 5369 (1973).
[34]M. Synek, A. E. Raines, and C. C. J. Roothaan, Phys. Rev. 141, 174 (1966).
[35]J. C. Slater and G. F. Koster, Phys. Rev. 94, 1498 (1954).
[36]R. C. Chaney, T. K. Tung, C. C. Lin, and E. E. Lafon, J. Chem. Phys. 52, 361 (1970).
[37]E. E. Lafon and C. C. Lin, Phys. Rev. 152, 579 (1966).
[38]J. G. Wills, Oak Ridge National Laboratory Report No. ORNL-TM-1949 (1967) (unpublished).
[39]J. Gell-Mann and K. A. Brueckner, Phys. Rev. 106, 364 (1957).
[40]K. S. Singwi, A. Sjölander, M. P. Tosi, and R. H. Land, Phys. Rev. B 1, 1044 (1970).
[41]J. W. McCaffrey, J. R. Anderson, and D. A. Papaconstantopoulos, Phys. Rev. B 7, 674 (1973).
[42]G. Lehmann and M. Taut, Phys. Status Solidi B 54, 469 (1972).
[43]G. Gilat and L. J. Raubenheimer, Phys. Rev. 144, 390 (1966).
[44]G. Gilat, J. Comp. Phys. 10, 432 (1972).
[45]See for example W. A. Harrison, *Solid State Theory*, (McGraw-Hill, New York, 1970), p. 239.
[46]See, for example, C. Kittel, *Quantum Theory of Solids* (Wiley, New York, 1963), p. 86.
[47]See for example S. Raimes, *The Wave Mechanics of Electron in Metals* (North-Holland, Amsterdam, 1967), p. 177.
[48]We see no fall to zero of the density of states at k_F in either the Hartree-Fock case or the correlated case. But this is an obvious contradiction since $\vec{\nabla}_{\vec{k}} E_c(\vec{k})$ possesses a singularity at k_F. If the density of states in the correlated case does not fall to zero, then there must exist a compensating singularity in the Hartree-Fock term $\vec{\nabla}_{\vec{k}} E_{\mathrm{HF}}(\vec{k})$ and the Hartree-Fock density must fall to zero at k_F. The contradiction is resolved by simply noting that the 89-point (LA) $\vec{k}$-space integration technique we use is incapable of resolving the very weak singularity in $\vec{\nabla}_{\vec{k}} E_c(\vec{k})$ or in $\vec{\nabla}_{\vec{k}} E_{\mathrm{HF}}(\vec{k})$. The singularity in $\vec{\nabla}_{\vec{k}} E_{\mathrm{HF}}(\vec{k})$ is thus as weak as or weaker than the singularity in $\vec{\nabla}_{\vec{k}} E_c(\vec{k})$.
[49]H. Ehrenreich and M. H. Cohen, Phys. Rev. 115, 786 (1959).
[50]M. Blume and R. E. Watson, Proc. Roy. Soc. A 270, 127 (1962).
[51]A. B. Kunz, D. J. Mickish, and T. C. Collins, Phys. Rev. Lett. 31, 756 (1973).
[52]L. D. Finkelshteyn and S. A. Nemnonov, Phys. Met. Metallogr. 38, 38 (1969).
[53]R. M. Jenkins and W. R. Datars, Phys. Rev. B 7, 2269 (1973).
[54]S. L. Altmann and A. P. Cracknell, Proc. Phys. Soc. 84, 761 (1964).
[55]R. A. Stager and H. G. Drickamer, Phys. Rev. 131, 2524 (1963).
[56]H. G. Drickamer, Solid State Physics 17, 1 (1965).
[57]S. L. Altmann, A. R. Harford, and R. G. Blake, J. Phys. F 1, 791 (1971).
[58]H. W. Skinner, T. G. Bullen and J. E. Johnston, Phil. Mag. 45, 1070 (1957).
[59]R. H. Kingston, Phys. Rev. 84, 944 (1951).
[60]For a discussion of these problems, see, for example, P. Best, Phys. Rev. B 3, 4377 (1971).
[61]P. O. Nilsson, G. Arbman, and D. E. Eastman, Solid State Commun. 12, 627 (1973).
[62]J. W. McCaffrey and D. A. Papaconstantopoulos, Solid State Commun. 14, 1055 (1974).
[63]For a graphic illustration of the Fermi surface suggested by experimental de Haas–van Alphen data see Fig. 4 in Ref. 53.
[64]L. M. Roberts, Proc. Phys. Soc. Lond. B70, 738 (1957).
[65]A. O. E. Animalu and V. Heine, Philos. Mag. 12, 1249 (1965).